Available online at www.sciencedirect.com
SCIENCE DIRECT®

Journal of the European Ceramic Society 24 (2004) 603–612

www.elsevier.com/locate/jeurceramsoc

Point defects and deviation from stoichiometry in $(Zn_{x-y/4}Mn_{1-x-3y/4}Fe_{2+y})_{1-\delta/3}O_4$

Jörg Töpfer[a], Rüdiger Dieckmann[b,*]

[a]*Department of Materials Science and Engineering, Fachholchschule Jena, Carl-Zeiss-Promenade 2, 07745 Jena, Germany*
[b]*Department of Materials Science and Engineering, Cornell University, Bard Hall, Ithaca, NY 14853-1501, USA*

Received 15 November 2002; received in revised form 17 March 2003; accepted 6 April 2003

Abstract

The deviation from stoichiometry, δ, in the spinel $(Zn_{x-y/4}Mn_{1-x-3y/4}Fe_{2+y})_{1-\delta/3}O_4$ with $x=0.25$ was measured thermogravimetrically at 1200 °C as a function of the oxygen activity, a_{O_2} and the cationic composition, y. Point defect thermodynamic modeling of the oxygen activity dependence of δ suggests that cation vacancies are the majority ionic defects at high oxygen activity and that cation interstitials dominate at lower activities. For the spinel with $x=0.25$ and $y=0.08$ the deviation from stoichiometry was measured also at 900, 1000 and 1100 °C. The variation of the majority defect population with temperature for the latter spinel composition, which is typical for technical soft ferrites, is discussed and enthalpies for defect formation reactions are estimated. The upper limit of the stability field of this ferrite at 1200 °C is determined. Implications of the variation of the phase stability field and the deviation from stoichiometry, δ, for the sintering regimes of soft ferrites are addressed.

Keywords: Ferrites; Non-stoichiometry; Point defects; (Zn, Mn)Fe_2O_4

1. Introduction

Soft ferrites emerged as an important class of magnetic materials several decades ago.[1,2] Mn–Zn ferrites are the standard ferrite materials for many high frequency applications, i.e. low loss power ferrites for switch-mode power supplies (SMPS) or high permeability ferrites for wide band and pulse transformers. These ferrites are produced worldwide on a large scale.

The composition dependence of the magnetization of Mn–Zn ferrites of the type $Zn_xMn_{1-x}Fe_2O_4$ has been studied by Gorter[3] and it was found that the introduction of diamagnetic Zn ions increases the magnetization. Typical soft ferrite compositions contain more than 50 mol% Fe_2O_3, i.e. the spinel composition can be described by the formula $(Zn_xMn_{1-x})_{1-y}Fe_{2+y}O_4$. The excess iron oxide is added to optimize the magnetic properties of the ferrites. Spinel compositions with excess iron oxide possess zero magneto-crystalline anisotropy due to the compensating effect of the Fe^{2+} ion's anisotropy[4] as well as a minimum magnetostriction. Both properties are essential prerequisites to optimize the permeability of the material.[5,6]

The usual manufacturing route for soft ferrites is a typical ceramic process that includes premixing, calcination, fine-milling, spray-drying, compaction and sintering. Sintering of Mn–Zn ferrites is performed at high temperatures in air at atmospheric pressure or at other high oxygen activities ($\log a_{O_2} \approx -1.5$ to -0.68); cooling of the ceramics has to be accompanied by a reduction of the oxygen activity in order to avoid decomposition of the spinel. A classical study by Blank[7] on quenched samples established the phase boundary of the spinel field. Blank also determined the concentration of Fe^{2+} ions in the samples by chemical titration and was the first to suggest lines of constant ferrous ion content in a $\log a_{O_2}$ vs. temperature diagram. Oxygen partial pressure diagrams of Mn–Zn-ferrites compiled on the basis of results from thermogravimetric experiments show that, for example, for a given temperature, the oxygen

* Corresponding author. Tel.: +1-607-255-4315; fax: 1-607-255-2365.
E-mail address: dieck@ccmr.cornell.edu (R. Dieckmann).

0955-2219/03/$ - see front matter © 2003 Elsevier Ltd. All rights reserved.
doi:10.1016/S0955-2219(03)00246-2

activity within the spinel phase field varies over several orders of magnitude coupled with a non-stoichiometry and a change in the Fe^{2+}-concentration in the samples.[8–11] Based on these data sintering of soft ferrites is often referred to as Blank curves sintering, i.e. the oxygen activity is varied with temperature according to an equation of the type

$$\log a_{O_2} = A - \frac{B}{T(K)} \quad (1)$$

where A and B are system-specific constants. Therefore, to better manipulate the electromagnetic properties of Mn–Zn-ferrites it is essential to precisely control the defect equilibria during sintering and cooling of these soft ferrite magnets. Only a few studies on the defect chemistry of Mn–Zn ferrites have been published so far. In the early literature[7–9] the non-stoichiometry of the samples is discussed as being coupled to the Fe^{2+}/Fe^{3+} ratio. The formation of cation vacancies was assumed in the investigation of redox equilibria[10] and in an early Fe tracer diffusion study.[12] The formation of oxygen vacancies also has been speculated on.[13]

Recently, electrical conductivity and total cation transference numbers have been measured as a function of temperature and oxygen activity for $Mn_{0.54}Zn_{0.35}Fe_{2.11}O_4$,[14] and data for the phase stability field of the spinel have been derived. It was shown that ionic transference numbers vary with the oxygen activity with an exponent of $+2/3$ or $-2/3$, depending on the oxygen activity range. This behavior is very similar to that observed for cation diffusivities in substituted Fe-spinels[15–17] and is attributed to different majority point defect regimes: cation vacancies at high oxygen activity and cation interstitials at low oxygen activity govern the cationic motion. Cation tracer diffusion experiments as a function of oxygen activity at 1200 °C[18] for $(Zn_xMn_{1-x-y}Fe_{2+y})_{1-\delta/3}O_4$ have confirmed this interpretation. However, an exact determination of the deviation from stoichiometry, δ, and an analysis of the majority ionic point defects in Mn–Zn ferrites have not yet been reported.

The deviation from stoichiometry, δ, and the majority defects in substituted Fe-spinels of the type $(Co,Fe,Mn)_3O_4$ have been systematically studied.[15,19–21] It has been shown that, in general, the deviation from stoichiometry, δ, displays an S-shaped curvature as a function of the logarithm of the oxygen activity and is accommodated as cation vacancies at high and cation interstitials at low oxygen activity with the stoichiometric spinel in between.

Recently, we have reported data for the deviation from stoichiometry, δ, and for the concentration of majority defects in $(Zn_xMn_{1-x}Fe_2)_{1-\delta/3}O_4$ for $0 \leqslant x \leqslant 0.5$.[22] It was found that the general evolution of δ with $\log a_{O_2}$ is similar to other substituted ferrite spinels. In this work, thermogravimetric measurements were performed to determine values for the deviation from stoichiometry, δ, as a function of oxygen activity at 1200 °C in a series of spinel ferrites of the type $(Zn_{x-y/4}Mn_{1-x-3y/4}Fe_{2+y})_{1-\delta/3}O_4$ with $x = 0.25$ and $0 < y < 0.10$, which are characterized by a composition with more than 50 mol% Fe_2O_3. As mentioned above, such compositions are typical for soft ferrites with interesting magnetic properties. We have identified the type of the majority defects by modelling the dependence of the deviation from stoichiometry, δ, from the oxygen activity with defect thermodynamics. For the spinel with $x = 0.25$ and $y = 0.08$ the deviation from stoichiometry, δ, was measured at 900, 1000, 1100 and 1200 °C and the enthalpies of defect formation reactions were obtained from the temperature dependence of the defect formation equilibrium constants. Moreover, the limits of the stability field of that ferrite were re-examined with the goal to more precisely establish the spinel stability limits.

2. Experiments

2.1. Sample preparation

Samples were prepared according to the standard ceramic technique. Fe_2O_3, Mn_3O_4 and ZnO (analytical grade) were wet homogenized. After drying, the powders were calcined at 1050 °C for 2 h. Next, the powders were fine-milled on a planetary ball mill to a mean particle size of 2−3 μm. After drying, granulation and addition of polyvinyl alcohol as a binder the powders were compacted. The pellets were sintered at 1300 °C for 20 h in air and quenched in water. Some of the pellets were milled to fine powder and the presence of a single spinel phase was confirmed by XRD. The grain size of the polycrystalline samples used for the thermogravimetric studies was about 20 μm.

2.2. Measurements of changes in the deviation from stoichiometry

The approximate spinel phase stability region for $Zn_xMn_{1-x}Fe_2O_4$ at 1200 °C was estimated to be between $-0.5 < \log a_{O_2} < -7$ based on data reported in Refs. 23 and 24 Changes in the deviation from stoichiometry, δ, were measured thermogravimetrically as a function of the oxygen activity within the limits of the spinel phase field for $(Zn_{x-y/4}Mn_{1-x-3y/4}Fe_{2+y})_{1-\delta/3}O_4$ with $x = 0.25$ for $0 \leqslant y \leqslant 0.10$ at 1200 °C. The variation of the deviation from stoichiometry of the spinel with $y = 0.08$ was measured at 900, 1000, 1100 and 1200 °C. Estimates for the limits of the phase field were taken from Refs. 7, 8 and 14.

A high-resolution microbalance (symmetrical set-up, total pressure in the balance about 0.5 atm, noise level

in flowing gases about 1 μg) was used to in-situ measure the mass changes of samples with different composition, y, after sudden changes of the oxygen activity. The samples were placed in a special alumina sample holder on alumina needles to minimize the contact area between sample and sample holder. Oxygen activities were established with gas-mixing pumps using N_2/O_2- or $CO/CO_2/N_2$-mixtures and measured in-situ next to the samples with zirconia-based electrochemical cells. Changes in the deviation from stoichiometry, $\Delta\delta$, that are associated with an uptake or release of oxygen, were measured by consecutive changes of the oxygen activity from a selected reference activity to another activity and back to the reference activity to check for the reversibility of the accompanying mass change, Δm, before changing to the next oxygen activity. From the recorded values of Δm, changes in the deviation from stoichiometry, $\Delta\delta$, were calculated as described later.

At high Zn-concentration and low oxygen activities, the measurements were severely influenced by the fast evaporation of Zn-species and at some conditions not possible at all. In the latter cases, the experiments were not continued towards lower oxygen activities and the investigation of the low oxygen activity phase boundary of the spinel stability field was then impossible. It has been shown that Mn–Zn ferrites lose ZnO at high temperature with a predominant vaporization of Zn[25] leading to a depletion of Zn ions in near-surface regions. Observations on the influence of this effect on the microstructure of sintered ferrites have been reported in Ref. 26.

3. Results

The mass changes, Δm, measured after oxygen activity jumps, and the corresponding changes of the deviation from stoichiometry, $\Delta\delta$, at 1200 °C as a function of oxygen activity for $x=0.25$ and $y=0$, 0.04, 0.06, 0.08 and 0.10, respectively, are reported in Table 1. This table contains additional data for $y=0.08$ at lower temperatures, 900, 1000 and 1100 °C. The values listed for $\Delta\delta$ were calculated by using the following equation

$$\Delta\delta = \delta - \delta^{o} = \frac{\Delta m}{m^{o}} \cdot \left(\frac{9M_{Me}}{4M_{O}} + 3 \right) \quad (2)$$

where $M_{Me}=(1/3)\cdot[(x-y/4)\cdot M_{Zn}+(1-x-3y/4)\cdot M_{Mn}+(2+y)\cdot M_{Fe}]$. M_{Zn}, M_{Mn} and M_{Fe} are the molar masses of zinc, manganese and iron, respectively, and m^{o} is the initial sample mass. Absolute values of the deviation from stoichiometry, δ, were obtained by fitting Eq. (3) to the experimental data, $\Delta\delta$, for different oxygen activities and constant cationic composition. This equation reads

$$\Delta\delta = \delta - \delta^{o} = [V]^{0} \cdot a_{O_2}^{2/3} - [I]^{0} \cdot a_{O_2}^{-2/3} - \delta^{o} \quad (3)$$

where δ^{o} is the deviation from stoichiometry at the reference oxygen activity. The theoretical background of Eq. (3) will be discussed in Section 4.

The resulting values for the deviation from stoichiometry, δ, in spinels of the type $(Zn_{x-y/4}Mn_{1-x-3y/4}Fe_{2+y})_{1-\delta/3}O_4$ at 1200 °C are shown in Fig. 1 a–e. The additional data obtained for δ for the spinel denoted above with $x=0.25$ and $y=0.08$, i.e. $Zn_{0.23}Mn_{0.69}Fe_{2.08}O_4$, at 900, 1000 and 1100 °C are displayed in Fig. 2a–c. The solid curves in Figs. 1 and 2 were drawn by fitting Eq. (3) to the experimental data; the fits were non-linear least squares fits.

The values extracted for $[V]^{o}$ and $[I]^{o}$ by fitting Eq. (3) to the experimental data for the variation of the oxygen content are reported in Table 2. The composition dependence of $[V]^{o}$ and $[I]^{o}$ at 1200 °C is shown in Fig. 3. Fig. 4 gives the temperature dependence of $[V]^{o}$ and $[I]^{o}$ for $Zn_{0.23}Mn_{0.69}Fe_{2.08}O_4$.

During our measurements we observed that the data available from the literature for the stability limit of $Zn_{0.23}Mn_{0.69}Fe_{2.08}O_4$ towards higher oxygen activities seem to be incorrect to some extent. Therefore we extended oxygen activity jumps in the direction of higher oxygen activities until we observed suddenly very large mass changes, indicating the formation of sesquioxide. An example for the observed mass changes at high oxygen activities including such outside of the spinel stability range is shown in Fig. 5. The upper spinel stability limit must be between the last oxygen activity investigated within the stability field and the first oxygen activity outside of the stability field where a very large mass change occurred. These oxygen activities are reported in Table 3 together with values estimated for the stability limit. Fig. 6 shows the location of all measured data points within the spinel stability range in the phase diagram for Fe-rich Mn–Zn ferrites in comparison with data from the literature for stability limits and the data derived for the upper stability limit.

4. Discussion

Point defect equilibria in magnetite, $Fe_{3-\delta}O_4$,[27,28] and in hausmannite, $Mn_{3-\delta}O_4$,[29] have been studied in great detail. The basic findings were that the majority defects are cation vacancies at high oxygen activities and cation interstitials at low oxygen activities. Oxygen vacancies and oxygen interstitials, if present in any significant concentration, are minority defects only. These conclusions have been shown to be valid also

Table 1
Measured mass changes, Δm, and corresponding changes of the deviation from stoichiometry, $\Delta\delta$, as a function of the oxygen activity in $(Zn_{x-y/4}\ Mn_{1-x-3y/4}Fe_{2+y})_{1-3/\delta}O_4$

$\log a_{O_2}$	Δm (μg)	$\Delta\delta 10^3$
(a)[a] $x=0.25$, $y=0$, $m^o=482.4$ mg, $T=1200$ °C		
−0.27	676	15.321
−0.58	460	10.426
−0.98	262	5.938
−1.28	148	3.354
−1.41	120	2.719
−1.58	80	1.813
−1.80	40	0.907
−2.24	0	0
−2.56	−21	−0.476
−2.77	−28	−0.635
−3.10	−40	−0.907
−3.16	−43	−0.974
−4.26	−45	−1.020
−5.05	−64	−1.450
(b)[b] $x=0.25$, $y=0.04$, $m^o=460.4$ mg, $T=1200$ °C		
−0.27	776	18.423
−0.51	554	13.152
−0.98	326	7.739
−1.28	198	4.700
−1.58	107	2.540
−1.80	70	1.662
−1.74	64	1.519
−2.24	0	0
−2.59	−35	−0.830
−2.81	−38	−0.902
−3.58	−71	−1.685
−4.07	−67	−1.590
−4.54	−100	−2.374
−5.74	−170	−4.036
(c)[c] $x=0.25$, $y=0.06$, $m^o=466.6$ mg, $T=1200$ °C		
−0.22	788	18.456
−0.52	569	13.327
−0.92	339	7.940
−1.22	212	4.965
−1.75	66	1.546
−2.22	0	0
−2.84	−40	−0.937
−3.64	−69	−1.616
−4.11	−67	−1.569
−4.91	−108	−2.529
−5.69	−140	−3.279
(d)[d] $x=0.25$, $y=0.08$, $m^o=475.0$ mg, $T=1200$ °C		
−0.22	987	22.705
−0.53	685	15.758
−0.92	394	9.064
−1.22	242	5.567
−1.75	75	1.725
−2.22	0	0
−2.86	−56	−1.288
−3.60	−78	−1.794
−3.67	−67	−1.541
−4.35	−88	−2.024
−5.49	−138	−3.174
(e)[e] $x=0.25$, $a=0.08$, $m^o=475.0$ mg, $T=1100$ °C		
−0.92	1011	23.257
−1.23	715	16.448
−1.36	610	14.032
−1.53	482	11.088
−1.65	370	8.511
−1.75	346	7.959
−1.93	260	5.981
−1.99	231	5.314
−2.33	140	3.220
−2.88	0	0
−3.41	−51	−1.173
−3.77	−65	−1.495
−5.28	−100	−2.300
−6.43	−120	−2.760
−6.95	−110	−2.530
(f)[f] $x=0.25$, $y=0.08$, $m^o=475.0$ mg, $T=1000$ °C		
−1.63	1057	24.315
−1.93	748	17.207
−2.23	511	11.755
−2.48	368	8.465
−2.61	273	6.280
−2.89	152	3.496
−3.33	24	0.552
−3.47	0	0
−3.63	−32	−0.276
−3.88	−62	−0.966
−5.47	−120	−1.840
−7.24	−125	−2.415
−8.29	−137	−3.151
(g)[g] $x=0.25$, $y=0.08$, $m^o=475.0$ mg, $T=900$ °C		
−3.23	344	7.913
−3.45	212	4.877
−3.89	0	0
−4.08	−88	−2.024
−4.34	−148	−3.405
−4.64	−193	−3.979
−6.70	−255	−5.866
−9.23	−253	−5.820
(h)[h] $x=0.25$, $y=0.10$, $m^o=455.2$ mg, $T=1200$ °C		
−0.22	1019	24.457
−0.52	727	17.449
−0.92	430	10.320
−1.23	271	6.504
−1.75	86	2.064
−2.22	0	0
−2.85	−56	−1.344
−3.66	−108	−2.592
−4.09	−108	−2.592
−4.95	−138	−3.312
−5.72	−168	−4.032

[a] From fitting: $\delta^o=(7.45\pm0.91)\times10^{-4}$.
[b] From fitting: $\delta^o=(9.03\pm1.49)\times10^{-4}$.
[c] From fitting: $\delta^o=(8.70\pm2.13)\times10^{-4}$.
[d] From fitting: $\delta^o=(10.93\pm1.99)\times10^{-4}$.
[e] From fitting: $\delta^o=(10.71\pm2.35)\times10^{-4}$.
[f] From fitting: $\delta^o=(13.69\pm2.48)\times10^{-4}$.
[g] from fitting: $\delta^o=(54.04\pm2.21)\times10^{-4}$.
[h] From fitting: $\delta^o=(12.36\pm2.89)\times10^{-4}$.

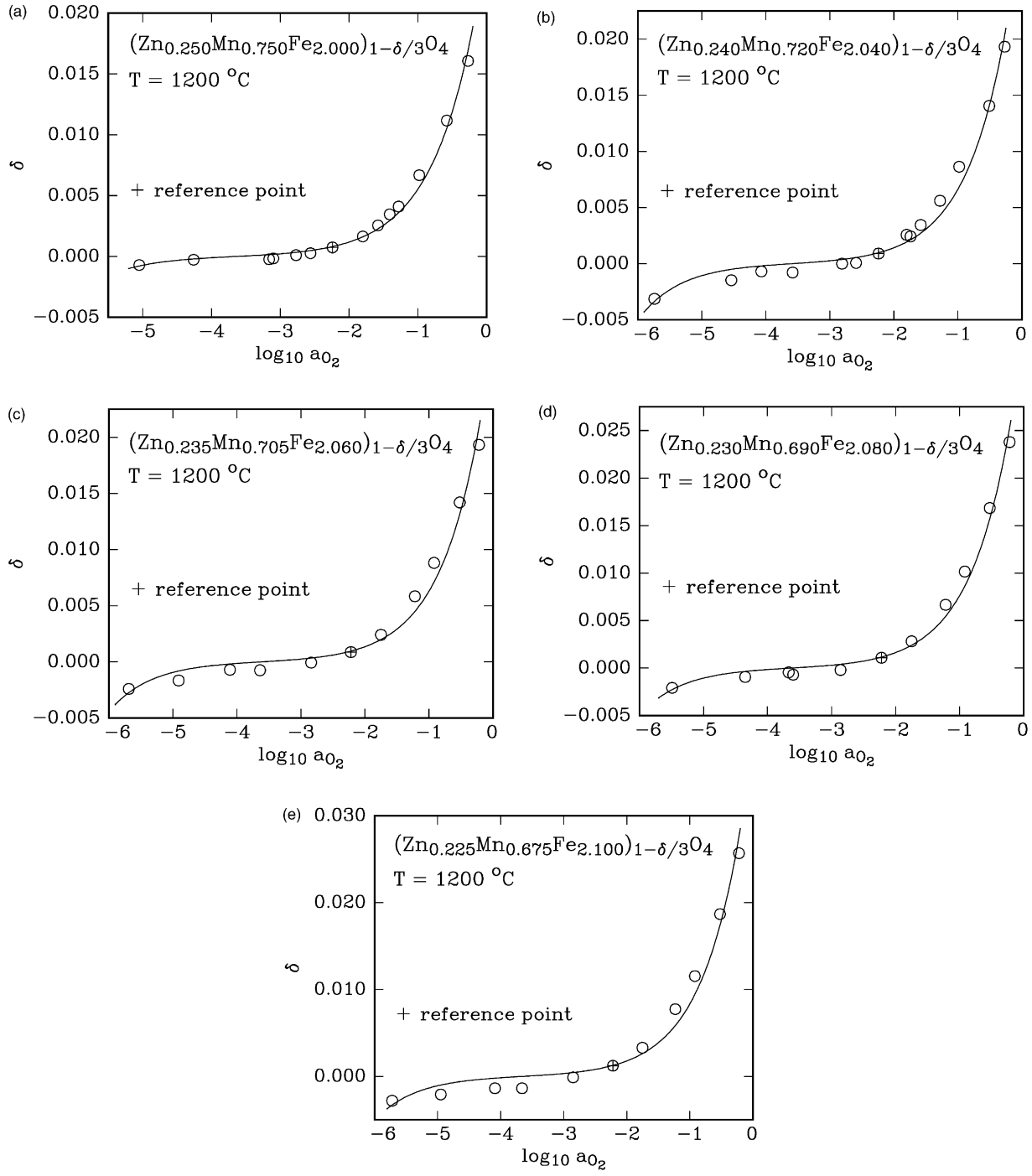

Fig. 1. Deviation from stoichiometry, δ, in $(Zn_{x-y/4x}Mn_{1-x-3y/4}Fe_{2+y})_{1-\delta/3}O_4$ with $x=0.25$ and $0\leqslant y\leqslant 0.10$ at 1200 °C as a function of the oxygen activity: (a) $y=0$, (b) $y=0.04$, (c) $y=0.06$, (d) $y=0.08$, and (e) $y=0.10$.

for magnetite-based solid solutions, see, for example, Refs. 15 and 17, as well as for Mn–Zn-ferrites with $y=0$ Ref. 22.

Cation vacancies are formed by the following reaction:

$$3Me_{Me}^{2+}+\frac{2}{3}O_2(g)\rightleftarrows 2Me_{Me}^{3+}+V_{Me}+\frac{1}{3}Me_3O_4(srg) \quad (4)$$

The notations used in this equation deviate from standard Kröger–Vink notations, see Ref. 30, because it is in spinels at high temperatures impossible to associate a distinct charge with a distinct cation site. The reason for this is the temperature-dependent cation distribution in spinels. Me_{Me}^{2+} denotes a metal ion with the charge 2+ on a cation site and Me_{Me}^{3+} such an ion with the charge 3+. V_{Me} is a vacancy on a cation site and $Me_3O_4(srg)$ is a molecular spinel building unit at a site of repeatable growth. Assuming that the concentration of Me^{3+} ions, $[Me_{Me}^{3+}]$ is about 2 and that

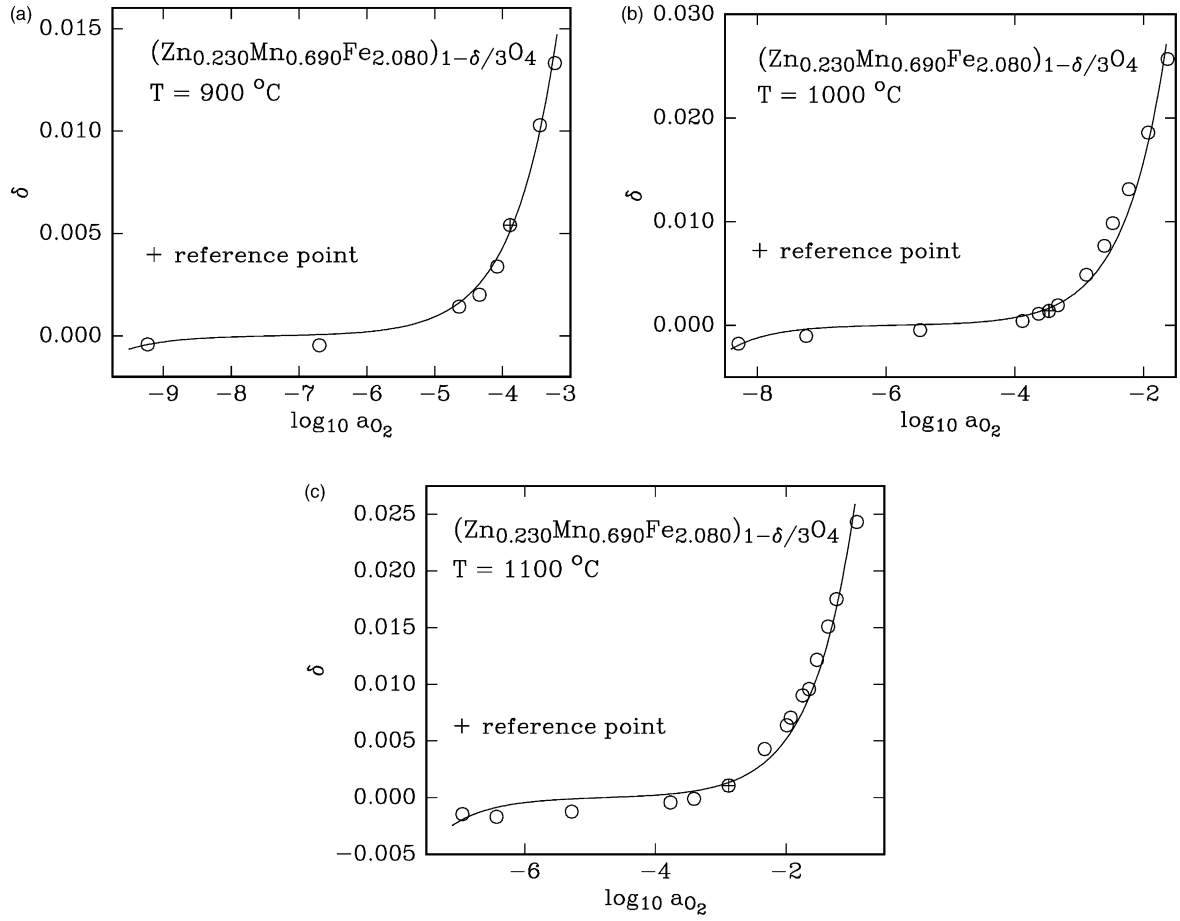

Fig. 2. Deviation from stoichiometry, δ, in $(Zn_{x-y/4}Mn_{1-x-3y/4}Fe_{2+y})_{1-\delta/3}O$ with $x=0.25$ and $y=0.08$, i.e., in $(Zn_{0.23}Mn_{0.69}Fe_{2.08})_{1-\delta/3}O_4$, at different temperatures as a function of the oxygen activity: (a) 900 °C, (b) 1000 °C, and (c) 1100 °C. Note: Fig. 1(d) gives the deviation from stoichiometry of $(Zn_{0.23}Mn_{0.69}Fe_{2.08})_{1-\delta/3}O_4$ at 1200 °C.

Table 2
Defect constants for cation vacancies, $[V]^o$, and cation interstitials, $[I]^o$, for $(Zn_{x-y/4}Mn_{1-x-3y/4}Fe_{2+y})_{1-3/\delta}O_4$ with $x=0.25$

y	T (°C)	log $[V]^o$	log $[I]^o$
0.00	1200	−1.59 + 0.01	−6.47 + 0.21
0.04	1200	−1.51 ± 0.01	−6.30 ± 0.08
0.06	1200	−1.53 ± 0.01	−6.35 ± 0.12
0.08	1200	−1.45 + 0.01	−6.30 + 0.15
0.08	1100	−0.95 ± 0.01	−7.35 ± 0.21
0.08	1000	−0.47 ± 0.01	−8.24 ± 0.22
0.08	900	0.30 ± 0.02	−9.52 ± 0.49
0.10	1200	−1.41 ± 0.02	−6.30 ± 0.14

Table 3
Measured oxygen activities and estimation of the upper spinel stability field phase boundary for $(Zn_{0.23}Mn_{0.69}Fe_{2.08})_{1-3/\delta}O_4$. nm = not measured

	900 °C	1000 °C	1100 °C	1200 °C
Highest measured log a_{O_2} within the spinel field	−3.23	−1.63	−0.92	−0.22
Lowest measured log a_{O_2} above the spinel field	−3.08	−1.45	−0.18	Nm
Estimated log a_{O_2} of upper boundary of spinel field	−3.15	−1.55	−0.5	0

$[Me^{2+}_{Me}]$ is about 1, the cation vacancy concentration can be expressed as:

$$[V_{Me}] = [V]^o \cdot a_{O_2}^{2/3} \quad (5)$$

Cation interstitials are formed via a Frenkel equilibrium reaction:

$$Me^{n+}_{Me} + V_I \rightleftarrows Me^{n+}_I + V_{Me} \quad (6)$$

Replacing the cation vacancy concentration in the mass action law of this reaction by Eq. (4) leads to the following oxygen activity dependence of the concentration of cation interstitials:

$$\left[Me^{n+}_I\right] = [I]^o \cdot a_{O_2}^{2/3} \quad (7)$$

Assuming that both defect types are the majority point defects (neglecting anionic defects) the deviation from stoichiometry, δ, can be expressed:

$$\delta = [V_{Me}] - \left[Me^{n+}_I\right] \quad (8)$$

Replacement of the concentrations of cation vacancies and interstitials by expressions containing the oxygen

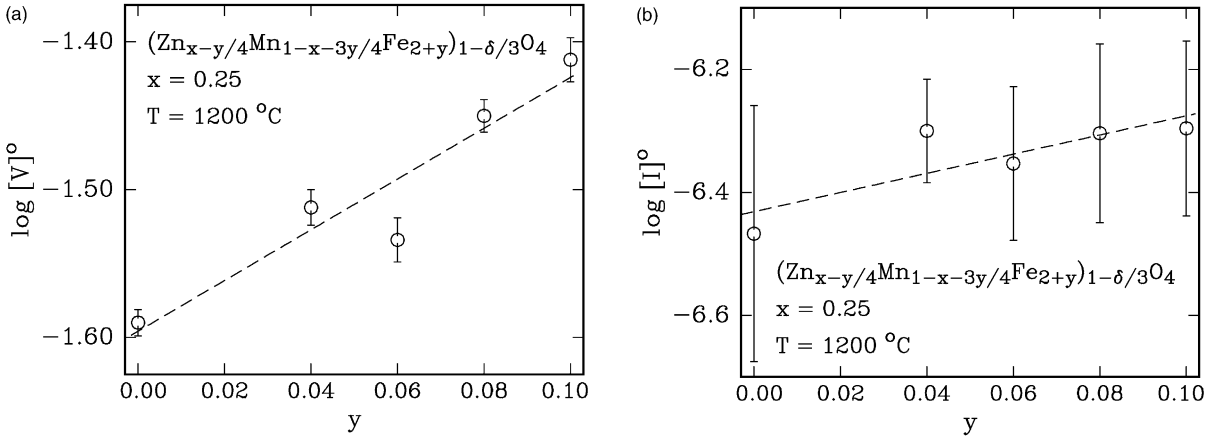

Fig. 3. Defect constants as a function of the cationic composition, y, in $(Zn_{x-y/4}Mn_{1-x-3y/4}Fe_{2+y})_{1-\delta/3}O_4$ with $x=0.25$ at 1200 °C: (a) for cation vacancies, $[V]^o$, and (b) for cation interstitials $[I]^o$.

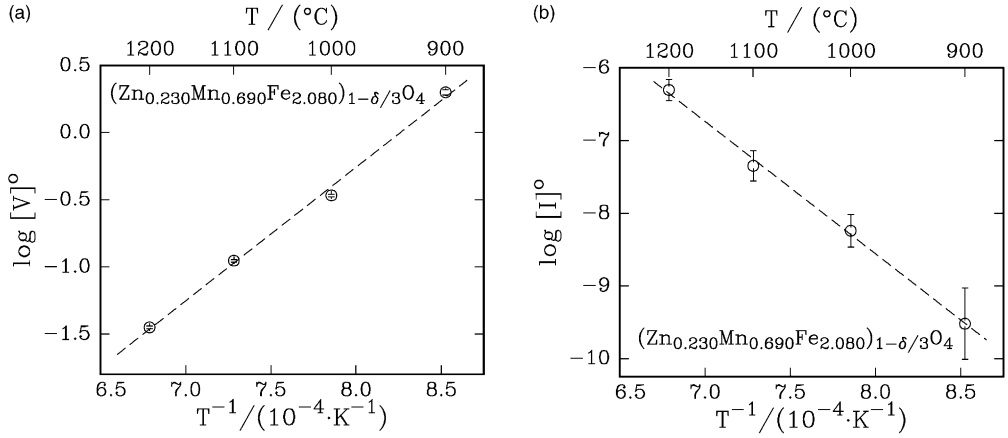

Fig. 4. Temperature dependence of defect constants for $(Zn_{0.23}Mn_{0.69}Fe_{2.08})_{1-\delta/3}O_4$: (a) for cation vacancies, $[V]^o$, and (b) for cation interstitials, $[I]^o$.

activity dependences of the concentrations of these defects, Eqs. (5) and (7), gives an oxygen activity dependence of δ of the form:

$$\delta = [V]^0 \cdot a_{O_2}^{2/3} - [I]^0 \cdot a_{O_2}^{-2/3} \quad (9)$$

with $[V]^o$ and $[I]^o$ as defect constants denoting the concentrations of cation vacancies and cation interstitials, respectively, normalized to $a_{O_2}=1$.

Eq. (9), rewritten as shown in Eq. (3), was fitted to the obtained data for $\Delta\delta$ as a function of the oxygen activity. From a non-linear least-squares fit, values for δ^o and for the defect constants $[V]^o$ and $[I]^o$ were extracted. The values obtained for δ^o were then used to calculate absolute deviations from stoichiometry, δ, which are shown in Figs. 1 and 2. In addition, S-shaped curves for δ as a function of log a_{O_2} were derived by using Eq. (9) and the values determined for $[V]^o$ and $[I]^o$. At higher oxygen activities the first term of Eq. (9) and thus cation vacancies dominate the deviation from stoichiometry. At lower oxygen activities, cation interstitials prevail and the concentration of cation vacancies becomes negligible. At the inflection points of the δ vs. log a_{O_2} curves, the spinel has a stoichiometric composition, i.e. $\delta=0$.

For the series $(Zn_xMn_{1-x}Fe_2)_{1-\delta/3}O_4$ the defect constants $[V]^o$ and $[I]^o$ were shown to vary as a function of composition, x (Ref. 22); $[V]^o$ slightly decreases and $[I]^o$ increases by about two orders of magnitude with increasing x. This result was surprising since one would expect that both constants should be independent on x if Zn^{2+} substitutes for Mn^{2+} without changing the charge state of ions. The observed variations of the defect constants with x were therefore attributed to changes in the valence state of ions due to the reaction

$$Fe_{Me}^{2+} + Mn_{Me}^{3+} \rightleftarrows Fe_{Me}^{3+} + Mn_{Me}^{2+} \quad (10)$$

which is also coupled to changes in the cation distribution. In-situ Mössbauer studies on $(Mn_{0.2}Fe_{0.8})_3O_4$ (Ref. 31) and on quenched samples of $MnFe_2O_4$ (Ref. 32) had shown that the equilibrium reaction (10) is shifted to the right, suggesting that the majority of the Fe is in the Fe^{3+} state and most of the Mn is Mn^{2+}.

In the series $(Zn_{x-y/4}Mn_{1-x-3y/4}Fe_{2+y})_{1-\delta/3}O_4$ with $x=0.25$ $[V]^o$ slightly increases with increasing y, while $[I]^o$ remains practically constant, see Fig. 3. The first observation is in agreement with the fact that upon increasing y the concentration of Fe^{2+} is increased too. Thus, the formation of cation vacancies based on the oxidation of Fe^{2+} ions, see Eq. (4), is facilitated compared with the situation at $y=0$.

The sample with $y=0.08$ was studied in more detail because its composition is representative for technical soft ferrite formulations. The variation of the deviation from stoichiometry δ as a function of oxygen activity for various temperatures is shown in Fig. 2. The basic findings are (i) the maximum oxygen activity at which the spinel is thermodynamically stable decreases as the temperature is reduced, (ii) the value of the defect constant for the formation of cation vacancies increases with decreasing temperature, see Fig. 4a, and (iii) the value of the defect constant for the formation of cation interstitials is reduced with decreasing temperature, see Fig. 4b.

The stability limits of the ferrite with $x=0.25$ and $y=0.08$ are considered in the phase diagram shown in Fig. 6. Included are the upper and lower stability limits of the similar ferrite composition $Zn_{0.35}Mn_{0.54}Fe_{2.11}O_4$[14] as well as the upper stability limits determined by Blank for $Zn_{0.31}Mn_{0.57}Fe_{2.12}O_4$[7] and by Morineau and Paulus[8] for $Zn_{0.33}Mn_{0.59}Fe_{2.08}O_4$. The location of the upper stability limit for $Zn_{0.23}Mn_{0.69}Fe_{2.08}O_4$ was detected in our thermogravimetric experiments by a large mass change observed when crossing the oxygen activity of the phase boundary; this mass change is much larger than the mass changes (in the μg range) associated with the change in the deviation from stoichiometry δ in the spinel phase, see Table 1. As an example, for $T=1000$ °C and $y=0.08$, this mass change is plotted in Fig. 5. The oxygen activities of the upper phase boundary determined in our experiments are somewhat higher than those reported in Refs. 7, 8 and 14.

The variation of the defect constants $[V]^o$ and $[I]^o$ with temperature, see Fig. 4, corresponds to an Arrhenius-type temperature dependence. From the slopes in Fig. 4 a and b, the enthalpies of the formation of cation vacancies and interstitials, respectively, were calculated. For the formation of cation vacancies an enthalpy $\Delta H_{cv}=-190\pm8$ kJ/mol results (assuming for the purpose of data fitting a random error of 0.05 in the logarithms of the defect constants in addition to those listed in Table 2), which is comparable with values of −198 kJ/mol for $Fe_{3-\delta}O_4$ (Ref. 27) and -158 ± 25 kJ/mol for $(Mg_{0.66}Mn_{0.21}Fe_{2.13})_{1-\delta/3}O_4$ (Ref. 33). The formation of cation vacancies is an exothermic process and therefore is more and more suppressed with increasing temperature. On the other hand, the enthalpy of cation interstitial formation is $\Delta H_{ci}=352\pm39$ kJ/mol. For the formation of cation interstitials in $Fe_{3-\delta}O_4$ an activa-

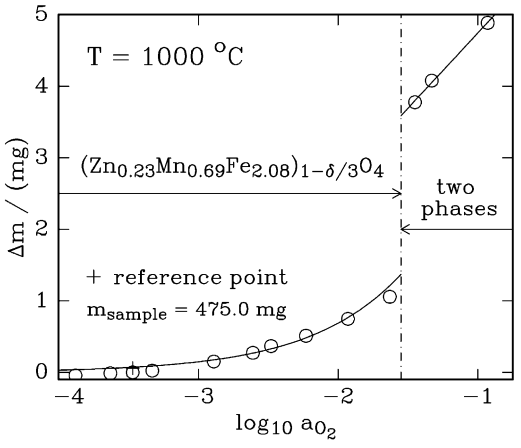

Fig. 5. Mass changes observed upon oxygen activity jumps towards higher oxygen activities for a sample of $Zn_{0.23}Mn_{0.69}Fe_{2.08}O_4$ (sample mass = 475.0 mg). The large step at very high oxygen activities indicates the formation of sesquioxide.

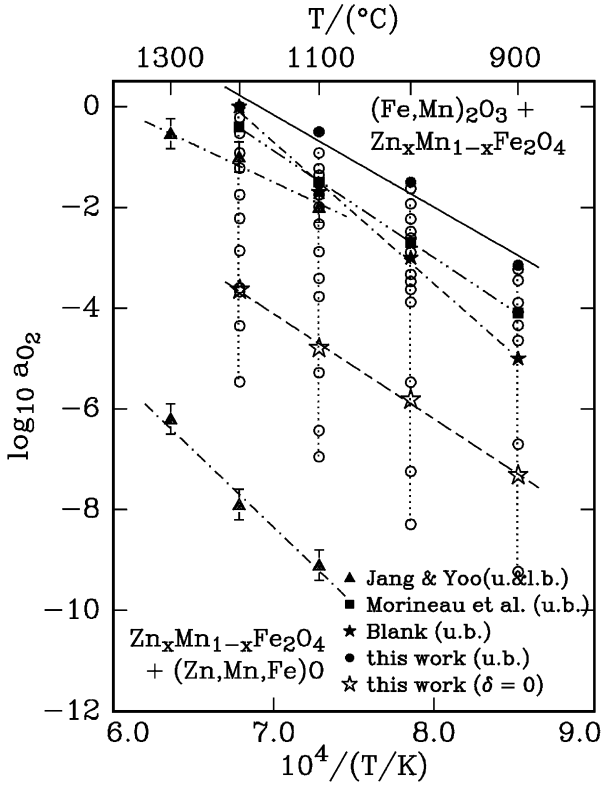

Fig. 6. Stability range of the spinel $Zn_{0.23}Mn_{0.69}Fe_{2.08}O_4$ as a function of temperature and oxygen activity. Data points from Ref. 14 for the upper and lower stability limits of $Zn_{0.35}Mn_{0.54}Fe_{2.11}O_4$: open triangles, data points from Ref. 7 for the upper stability limit of $Zn_{0.31}Mn_{0.57}Fe_{2.12}O_4$: filled stars, data point from Ref. 8 for the upper stability limit of $Zn_{0.33}Mn_{0.59}Fe_{2.08}O_4$: filled square, $\Delta\delta$ measured in this study at 900, 1000, 1100 and 1200 °C and at different oxygen activities: vertical dotted lines and open circles, oxygen activities determined in this study for the upper stability limit of the spinel $Zn_{0.23}Mn_{0.69}Fe_{2.08}O_4$: filled circles, and oxygen activities at which $\delta=0$, i.e. where the composition is exactly $Zn_{0.23}Mn_{0.69}Fe_{2.08}O_4$, calculated with Eq. (11): open stars.

tion enthalpy of 522 kJ/mol was found[27] and for the (Mg,Mn)-substituted ferrite denoted above a value of $\Delta H_{ci} = 416 \pm 6$ kJ/mol.[33] The cation interstitial formation is endothermic, and therefore the concentration of interstitials increases with increasing temperature. Interestingly, for the high temperature phase of hausmannite, β-$Mn_{3-\delta}O_4$, the formation of cation vacancies and of cation interstitials are both endothermic ($\Delta H_{cv} = 114$ kJ/mol and $\Delta H_{ci} = 427$ kJ/mol).[29] The sign of the enthalpy of cation vacancy formation seems to be related to the energetics of the oxidation of Me^{2+} cations to Me^{3+} cations. The fact that the cation vacancy formation in the Mn–Zn ferrite studied here is exothermic as in the case of magnetite suggests that the prevailing cation vacancy formation reaction is coupled to the oxidation of Fe^{2+} ions to Fe^{3+} ions.

With the data obtained for [V]° and [I]° as a function of temperature, the concentration of both majority defects in $(Zn_{0.23}Mn_{0.69}Fe_{2.08})_{1-\delta/3}O_4$ can be calculated as a function of temperature and oxygen activity. This is especially simple for the stoichiometric composition, i.e., for $\delta = 0$. From Eq. (9) it follows for the stoichiometric spinel

$$a_{O_2}(\delta = 0) = \left(\frac{[I]^o}{[V]^o}\right)^{3/4} \quad (11)$$

The values calculated for log a_{O_2} ($\delta = 0$) for the four temperatures studied are included in the phase diagram shown in Fig. 6 to distinguish between regions in which cation vacancies are the predominant defects, i.e. at $a_{O_2} > a_{O_2}$ ($\delta = 0$), and regions where cation interstitials prevail, i.e. at $a_{O_2} < a_{O_2}$ ($\delta = 0$). From Fig. 6 it follows that the oxygen activity of the stoichiometric spinel composition is shifted to lower values if the temperature is reduced. The oxygen activity at which the spinel is stoichiometric is given by the equation

$$\log a_{O_2}(\delta = 0) = \frac{(-2.09 \pm 0.07) \cdot 10,000}{T/(\mathrm{K})} + (10.5 \pm 0.5) \quad (12)$$

According to Eq. (12) the stoichiometric spinel $(Zn_{0.23}Mn_{0.69}Fe_{2.08})O_4$ is stable at log $a_{O_2} = -3.64$ at $T = 1200$ °C. This oxygen activity is considerably smaller than that reported by Tanaka[34] for the stoichiometric condition at 1200 °C.

The knowledge of the phase stability field of $(Zn_{0.23}Mn_{0.69}Fe_{2.08})_{1-\delta/3}O_4$ and of the data for the deviation from stoichiometry, δ, can be used to tailor routines for the sintering and cooling of such ferrites. Thus a control of the concentration of majority defects as well as of the concentration of Fe^{2+} is possible. The effect of δ and the ferrous iron content on the magnetic properties of Mn–Zn ferrites will be further investigated.

5. Conclusions

The deviation from stoichiometry, δ, was measured as a function of oxygen activity and cationic composition ($x = 0.25$, $y = 0$–0.10) in $(Zn_{x-y/4}Mn_{1-x-3y/y}Fe_{2+y})_{1-\delta/3}O_4$ at 1200 °C and for $y = 0.08$ at 900 to 1200 °C. S-shaped curves were observed in plots of δ vs. log a_{O_2}. Cation vacancies were identified as the majority defects at high oxygen activities, while cation interstitials dominate at low oxygen activities. The defect constant for cation vacancies, $[V]^o$, was found to increase with an increasing excess of iron, y, while the defect constant for cation interstitials, $[I]^o$, is practically independent of y.

Acknowledgements

The authors thank the US Department of Energy for support of this work under grant No. DE-FGO2-88ER45357. This work made use of the Cornell Center of Materials Shared Experimental Facilities, supported through the National Science Foundation Materials Research Science and Engineering Centers program (DMR-0079992). One of the authors (J.T.) is thankful for support by the Bundesministerium für Bildung und Forschung (BMBF, Germany) under grant no. 03N1069.

References

1. Smith, J. and Wijn, H. P. J., *Ferrite (Philips Technische Bibliothek)*. Centrex Verlag, Eindhoven, 1962.
2. Snelling, E. C., *Soft Ferrites: Properties and Applications*, 2nd edn. Butterworth & Co. Ltd, London, 1988.
3. Gorter, E. W., Saturation magnetization and crystal chemistry of ferrimagnetic oxides. *Philips Res. Repts.*, 1954, **9**, 321–365.
4. Ohta, K., Magnetocrystalline anisotropy and magnetic permeability of MnZnFe ferrites. *J. Phys. Soc. Japan*, 1963, **18**(5), 685–690.
5. Stoppels, D. and Boonen, P. G. T., The influence of the second-order magnetocrystalline anisotropy on the initial permeability of MnZn ferrous ferrites. *J. Magn. Magn. Mat.*, 1980, **19**, 409–411.
6. Ohta, K. and Kobayshi, N., Magnetostriction constants of MnZnFe Ferrites, Japn. *J. Appl. Phys.*, 1964, **3**(10), 576–580.
7. Blank, J., Equilibrium atmosphere schedules for the cooling of ferrites. *J. Appl. Phys.*, 1961, **32**(3), 378–379.
8. Morineau, R. and Paulus, M., Chart of P_{O_2} versus temperature and oxidation degree for Mn–Zn ferrites in the composition range: $50 < Fe_2O_3 < 54$; $20 < MnO < 35$; $11 < ZnO < 30$ (mole%). *IEEE Trans. Magn.*, 1975, **11**(5), 1312–1314.
9. Morineau, R. and Paulus, M., Oxygen partial pressures of Mn–Zn ferrite. *Phys. Stat. Sol. (a)*, 1973, **20**, 373–380.
10. Morineau, R., Structural defects and oxidation-reduction equilibrium in Mn–Zn-ferrites. *Phys. Stat. Sol. (a)*, 1976, **38**, 559–568.
11. Slick, P. I. and Basseches, H., Thermogravimetric study of the solid–gas interaction of a Mn–Zn ferrite and the effect on its magnetic properties. *IEEE Transactions on Magnetics*, 1966, **2**(3), 603–607.
12. Ogawa, S., Oxidation rate and phase diagram of Mn–Zn ferrite determined from the cation diffusion coefficient. *Japan. J. Appl. Phys.*, 1967, **6**(12), 1427–1433.

13. Inaba, H., Nonstoichiometry and its effect on the magnetic properties of a manganese–zinc ferrite. *J. Am. Ceram. Soc*., 1985, **78**(11), 2907–2912.
14. Jang, Y.-I. and Yoo, H.-I., Phase stability and ionic transference number of a ferrite spinel, $Mn_{0.54}Zn_{0.35}Fe_{2.11}O_4$. *Solid State Ionics*, 1996, **84**(1–2), 77–88.
15. Lu, F.-H. and Dieckmann, R., Point defects and cation tracer diffusion in $(Co,Fe,Mn)_{3-\delta}O_4$ spinels: I. Mixed spinels $(Co_xFe_{2y}Mn_y)_{3-\delta}O_4$. *Solid State Ionics*, 1992, **53–56**, 290–302.
16. Franke, P. and Dieckmann, R., Defect structure and transport properties of mixed iron–manganese oxides. *Solid State Ionics*, 1989, **32/33**(Part I), 817–823.
17. Töpfer, J., Aggarwal, S. and Dieckmann, R., Point defects and cation tracer diffusion in $(Cr_xFe_{1-x})_{3-\delta}O_4$ spinels. *Solid State Ionics*, 1995, **81**(3–4), 251–266.
18. Lee, J.-H., Martin, M. and Yoo, H.-I., Self- and impurity cation diffusion in manganese–zinc–ferrite, $Mn_{1-x-y}Zn_xFe_{2+y}O_4$. *J. Phys. Chem. Solids*, 2000, **61**(10), 1597–1605.
19. Lu, F.-H. and Dieckmann, R., Non-stoichiometry and cation tracer diffusion in cobalt-iron-manganese mixed oxide spinels, In *Point Defects Related Properties of Ceramics*, ed. T.O. Mason and J. Routbort. *Ceram. Trans*., 1991, **24**, 185–192.
20. Lu, F.-H. and Dieckmann, R., Point defects and cation tracer diffusion in $(Co,Fe,Mn)_{3-\delta}O_4$ spinels: II. Mixed spinels $(Co_xFe_zMn_{2z})_{3-\delta}O_4$. *Solid State Ionics*, 1993, **59**(1–2), 71–82.
21. Lu, F.-H. and Dieckmann, R., Point defects in oxide spinel solutions of the type $(Co,Fe,Mn)_{3-\delta}O_4$ at 1200 °C. *J. Phys. Chem. Solids*, 1995, **56**(5), 725–733.
22. J. Töpfer, R. Dieckmann. Deviation from stoichiometry and point defects in $(Zn_xMn_{1-x}Fe_2)_{1-\delta/3}O_4$. Solid State Ionics, (in press; article in press available at http://www.sciencedirect.com; *Solid State Ionics* 2003, **159**(3–4), 397–404.
23. P. Franke and R. Dieckmann, unpublished data.
24. Roth, R. S., Negas, T., Cook, L. P., ed., *Phase Diagrams for Ceramists, Vol. IV*. The American Ceramic Society, Columbus, OH, 1981.
25. Inaba, H. and Matsui, T., Vaporization and diffusion of Mn–Zn ferrite. *J. Solid State Chem*., 1996, **121**(1), 143–148.
26. Sainamthip, P. and Amarakoon, V. R. W., Role of zinc volatilization on the microstructural development of manganese zinc ferrites. *J. Am. Ceram. Soc*., 1988, **71**(8), 644–648.
27. Dieckmann, R., Defect and cation tracer diffusion in magnetite (iv): nonstoichiometry and point defect structure of magnetite $(Fe_{3-\delta}O_4)$. *Ber. Bunsenges. Phys. Chem*., 1982, **86**(2), 112–118.
28. Dieckmann, R. and Schmalzried, H., Defects and cation diffusion in magnetite (I). *Ber. Bunsenges. Phys. Chem*., 1977, **81**(3), 344–347.
29. Keller, M. and Dieckmann, R., Defect structure and transport properties of manganese oxides: (II) the nonstoichiometry of hausmannite $(Mn_{3-\delta}O_4)$. *Ber. Bunsenges. Phys. Chem*., 1985, **89**(10), 1095–1104.
30. Kröger, F. A. and Vink, H. J., Relations between the concentrations of imperfections in crystalline solids. In *Solid State Physics—Advances in Research and Applications, Vol. 3*, ed. F. Seitz and D. Turnbull. Academic Press, New York, 1957, pp. 307–435.
31. Becker, K. D., Pattanayak, J. and Wiβmann, S., A high-temperature Mössbauer study of the cation distribution in $(Fe,Mn)_3O_4$ Spinels. *Solid State Ionics*, 1994, **71/72**(Part I), 497–502.
32. Bonsdorf, G., Dehnecke, M. A., Schäfer, K., Christen, S., Langbein, H. and Gunβer, W., X-ray absorption spectroscopy and Mössbauer studies of redox and cation-ordering processes in manganese ferrite. *Solid State Ionics*, 1997, **101–103**, 351–357.
33. Kang, S.-H. and Yoo, H.-I., Nonstoichiometry and high-temperature thermodynamic properties of $(Mg_{0.22}Mn_{0.07}Fe_{0.71})_{3-\delta}O_4$ ferrite spinel. *J. Solid State Chem*., 1999, **145**(1), 276–282.
34. Tanaka, T., Equilibrium oxygen pressures of Mn–Zn ferrites. *J. Am. Ceram. Soc*., 1981, **64**(7), 419–421.